Research Article

Numerical and artificial neural network analyses of ground surface settlement of tunnel in saturated soil

Vahed Ghiasi[1] · Mehdi Koushki[2]

Abstract

The main purpose of this research is to predict the ground surface settlement in tunneling of a single circular tunnel with simultaneous changes in the mechanical properties of soil and geometrical properties of the tunnel section. In this research, numerical and parametric analysis of circular tunneling in frictional–cohesive saturated soil has been investigated using 2D finite element method by ABAQUS. In other words, the behavior of ground surface, considering to change the different values of depth-to-diameter ratio (H/D), soil cohesion, internal friction angle, permeability coefficient, and the influence of these variables on settlement of surface in each model, has been separately evaluated. Then, a multilayer perceptron (MLP) artificial neural network is designed to predict the ground surface settlement. MLP is a type of feed-forward artificial neural network utilizing backpropagation technique for training phase, and the Levenberg–Marquardt method is used to reduce the errors and the distance between the network outputs and finite element method results. There are some independent variables in the input layer and a dependent variable in the output layer. The middle layer consists of seven neurons. Finally, the high potential of the artificial neural network with a correlation coefficient of 0.98 is shown in the prediction of ground surface settlement.

Keywords Ground surface settlement · Finite element method · Multilayer perception artificial neural network

1 Introduction

In recent years, there has been an increasing interest in the tunnel construction [1–4]. Ground surface settlement due to tunneling is one of the inevitable problems in tunnel engineering. The long-term settlement and differential settlement of tunnels have led to serious longitudinal deformation. The deformation pattern of tunnels is the step between rings rather than by the beam/cylindrical shell bending. Most of the lining rings distort into the shape of a horizontal ellipse (tunnel squat), but a few acquire the shape of a vertical ellipse. Large tunnel deformation has caused groundwater infiltration and the separation of ballastless track bed and lining. Further analysis shows that long-term tunnel settlement is mainly due to urbanization induced land settlements in Shanghai. The magnitude of tunnel settlement is correlated with sublayer settlement rather than ground surface settlement. In the early operational years, post-construction settlement induced by tunneling and the cyclic loading of trains may contribute significantly to the tunnel settlement. However, at some special places, nearby construction and groundwater infiltration are responsible for the long-term settlement of the tunnel [5].

In the past few decades, as a new tool for analysis of the tough geotechnical problems, artificial neural networks (ANNs) have been successfully applied to address a number of engineering problems, including deformation due to tunneling in various types of rock mass. Unlike the classical regression methods in which a certain form for

✉ Vahed Ghiasi, v.ghiasi@malayeru.ac.ir; Mehdi Koushki, Mehdi.koushki70@gmail.com | [1]Faculty of Civil Engineering, Malayer University, Hamedan, Iran. [2]M.S. of Geotechnical Engineering, Malayer University, Hamedan, Iran.

the approximation function must be presumed, ANNs do not require the complex constitutive models. Additionally, it is traced that the ANN prediction system is one of the most effective ways to predict the rock mass deformation. Furthermore, it could be envisaged that ANNs would be more feasible for the dynamic prediction of displacements in tunneling in the future, especially if ANN models are combined with other research methods [6].

In this study, the ground surface settlement has been investigated by tunnel depth, diameter, internal friction angle, adhesion, and soil permeability coefficients. Then, by transferring the data obtained from ABAQUS, as input data to MATLAB and by creating a multilayer perceptron network, the ground surface settlement prediction model is designed. First, in 1958, Martos, and Peck in 1969 carried out their studies to model, calculate, and predict ground surface settlement during tunneling [7, 8]. Pack developed his model with respect to the inverse normal distribution model. According to this theory, the ground surface settlement is obtained from Fig. 1 and the following equation.

$$S_v = S_{max} e^{\frac{-x^2}{2i^2}} \tag{1}$$

where s is the vertical ground surface settlement at any point, S_{max} is the maximum settlement of ground surface on the tunnel axis, i is the horizontal distance of the tunnel axis from the turning point of the settlement curve, and x is the horizontal distance from the tunnel axis.

Thereafter, many researchers investigated and predicted the ground surface settlement and displacement, by modifying the parameters introduced by Pack et al. Research in this field can be divided into four categories. The first category is analytical studies that utilize relationships in soil and rock mechanics and combine them with mathematical foundations to predict the amount of settlement in single and twin circular tunnels [9–16]. Experimental and laboratory research falls into the second category. Most studies in this field are carried out by creating a tunnel element and its surroundings at a very smaller scale in

the laboratory environment than the actual element and utilizing a centrifuge system [17–20]. The next category of research is numerical studies. Most numerical studies using finite element methods and finite difference methods have investigated surface settlement and subterraneous displacement due to tunneling [21–29]. Finally, artificial intelligence research and neural networks are used in most studies today. The high accuracy and speed of computation in predicting different parameters, taking into account the maximum of independent variables affecting the parameter in question, have led to the increasing use of neural networks in different researches [30–35]. In this study, it has been tried to predict the ground surface settlement due to tunneling by combining two numerical methods and using artificial neural networks.

2 Problem definition

The two-dimensional model created using ABAQUS finite element software, which is highly capable of analyzing soil environments, is 40×80. The type of analysis used in this model is standard analysis. The general form of the model considered in this study is given in Fig. 2. This model includes a frictional–adhesive homogeneous soil. The parameters investigated in this study are listed in Table 1. Other geometrical and mechanical parameters of the tunnel, such as tunnel diameter and modulus of elasticity, are assumed to be constant. In fact, this study analyzed three separate situations in accordance with Fig. 1 and that presented in Table 1. The behavioral model considered for the soil is the Mohr–Coulomb model.

The mesh created for the value $H/D = 1$ is shown in Fig. 3. The model is divided into 5700 square corners. However, at points close to the tunnel section, the elements are rectangular in order to provide a more accurate analysis of the area. In both $H/D = 1$ and $H/D = 2$ models, in addition to the element geometry, the number of elements is equal to or near the number of

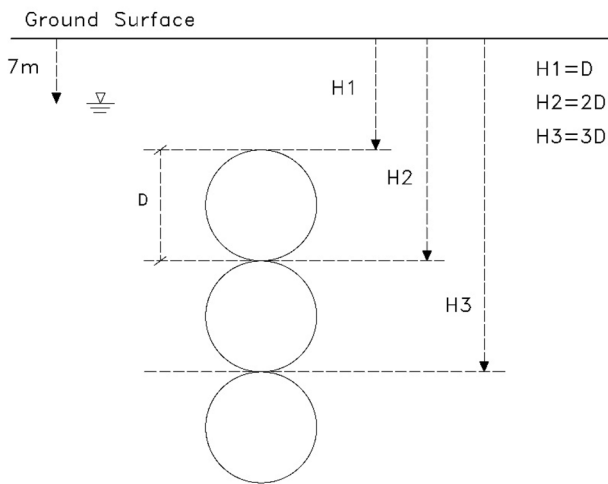**Fig. 1** Ground surface settlement above single tunnel described [8]
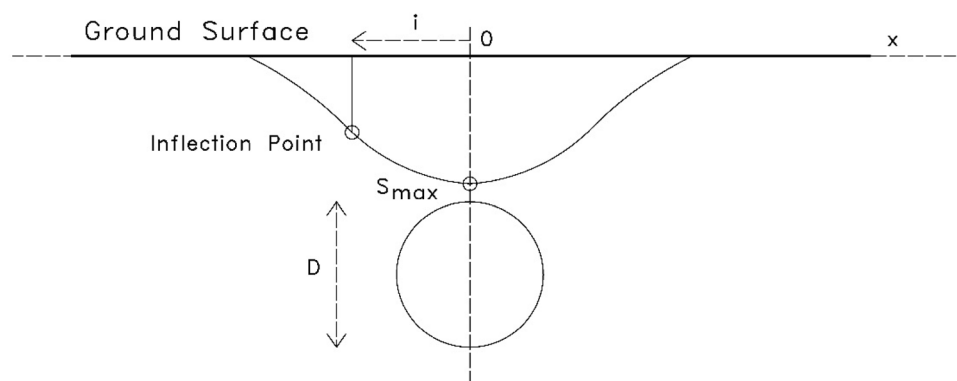
Fig. 2 Scheme of tunnel drilled in three depth modes

Table 1 Soil properties and used parameters [36]

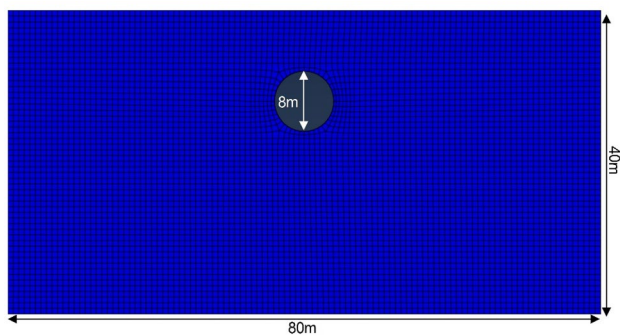| Parameter	Unit	Value
Dry unit weight	γ_d (KN/m^3)	17
Saturated unit weight	γ_{sat} (KN/m^3)	20.7
Young's modulus	E (kPa)	5000
Coefficient of permeability	k (m/s)	$1*10^{-8}$, $1*10^{-5}$, $1*10^{-2}$
Angle of internal friction	$\varphi(-)$	20, 30, 35, 40, 45
Cohesive strength	C (kPa)	20, 40, 60, 80
Poisson's ratio	$\nu(-)$	0.3

Fig. 3 Generally designed mesh in ABAQUS

elements in the first case. The finer elements are used in the surroundings of the tunnel section to increase the accuracy of the analysis. Also, the overall dimensions of the model are chosen to minimize the impact of lateral and lower boundaries. The groundwater level is selected 7 m below ground surface in all scenarios. As a result, in all the analyses, the tunnel drilling section is saturated. The mechanical properties of the soil with respect to φ

Table 2 Modeling mesh specifications

Type	Element type	Number of elements	Average size element (m)
Soil	15 nodded	4790	7.08 E−0.1

and C and in situ stresses are assumed to be effective, given the saturation of the environment. Also, the relation 2 was used to calculate the lateral coefficient in the soil.

$$k = 1 - \sin \varphi \qquad (2)$$

It should be noted that the amount of ground surface settlement is measured immediately after drilling. The analysis and measurement of settlements have been examined without considering the tools for tunnel stability. In fact, all the settlement values are obtained immediately after drilling.

In 2011, Yamamoto, in order to analyze the tunnel stability, using the upper and lower bound limit analysis method, which is considered one of the plastic analyses, obtained numbers as the stability number [36] and then similarly analyzed the tunneling settlements that used the Yamamoto method to utilize the upper and lower bound limit analysis [37]. The difference between the present study and the mentioned methods is considered the pore water pressure and soil saturation at the time of analysis.

Since the geometry of the model is complete, the finite element model, or mesh, is produced in Fig. 3.

(The program automatically generates the mesh and divides the geometric model according to the model structure into basic elements, according to which it fits the best base triangles in the model. Due to the fact that the analyses are performed in different phases, In all phases, an attempt has been made to select the coarseness mesh option and place the distribution element option on the fine every mode, and by reselecting the mass inside the tunnel and selecting a smaller mesh, the movement around the tunnel is calculated and observed more accurately. Specifications for the main model mesh are given in Table 2 (shown).

In general, all boundaries in each direction must have boundary conditions applied to them. If no boundary conditions are assigned to the model (free boundary), natural conditions apply. That is, the prescribed forces are equal to zero and the boundaries move freely. The software automatically sets a standard boundary to avoid the situation of indeterminate displacements, so that by designating reference points, the software completely rigs the horizontal boundary and by creating rolling boundaries in a vertical direction, it allows the soil to move and settle.

In this study, the urban tunnel with no overburden is considered at ground surface and the porosity ratio for the whole model is considered to be 0.58 with respect to its specific gravity and weight density of solid grains. The analysis is done in two steps. The first step includes entering the necessary information into the software, creating appropriate boundary conditions, and applying pore water pressures and effective in situ stresses in the soil model, and then, performing drilling operations, in which, immediately after drilling, ground surface settlement values are measured.

3 Results

Artificial neural network (ANN) is one of the scientific methods for predicting a variable through one or more other variables. Among the different methods of artificial neural networks is multilayer perceptron neural network, due to the use of post-diffusion algorithm. The method used in this study was used to calculate the error and reduce the error rate as much as possible and also to correct the error values by repeating the computational process.

In the study, after the set data required for network use were calculated and collected through finite element method software in 119 modes. A multilayered artificial neural network with a single input layer, the output layer and a hidden layer consisting of seven neurons or nodes was designed and built. Finally, the network is created by receiving three input variables, which include the diameter of the tunnel, the distance from the center to the center of the tunnel, and the depth of the center of the tunnel to the ground level, calculating the maximum subsidence value after passing through the network. The results indicate that the creation of a neural network, due to its very high speed and cost-effectiveness, is able to predict the surface subsidence resulting from the tunneling of twin tunnels.

The effect of the soil permeability coefficient and pore water pressure on the amount of ground surface settlement and soil displacement around the tunnel was investigated. As the permeability coefficient in the soil increased, the surface settlement due to tunneling decreased. According to the results obtained from H, as the ground depth increased, the higher the permeability coefficient in soil, the higher amount of surface settlement. However, as the angle of internal friction and adhesion in the soil increases, the intensity of this process is reduced, approaching the same trend for the other depths. Lowering the permeability beyond the values of a and b would have little effect on the surface settlement. Increasing the amount of adhesion in all the states and analyses has reduced the amount of ground surface settlement. Increasing the angle of internal friction of the soil, in most cases, has reduced the ground surface settlement. However, as soil adhesion increased simultaneously, this decreasing trend was less observed. In some cases, for larger adhesions up to 40 kPa, with increasing internal friction angle, the surface settlement has increased or been constant, which this trend has been observed more for tunnels closer to the surface. Ground surface settlement at different depths is completely dependent on the shear strength parameters of the soil. When the permeability coefficient is highest, and the internal friction angle of the soil was at its lowest, the surface settlement is a function of depth, which increased significantly with increasing depth. With increasing shear strength parameters, the dependence of ground surface settlement on depth is seen to be lower, so that when these parameters reach their maximum, it can be said that the surface settlement is independent of the depth of drilling.

4 Discussion

4.1 Investigation of the influence of permeability coefficient

One of the main objectives of this study is to investigate the effect of the soil permeability coefficient and pore water pressure on the amount of ground surface settlement and soil displacement around the tunnel environment. By investigating the changes in soil permeability, according to Table 3 and Fig. 4, with increasing soil permeability coefficient, the amount of ground surface settlement due to tunneling has decreased. This trend is clearly seen in the values obtained for $H/D = 1$. The results for $H/D = 2$ and $H/D = 3$ in most cases illustrate this trend. With increasing depth, the angle of internal friction and adhesion in soil increased, and the inverse relationship between soil permeability coefficient and ground surface settlement was more pronounced.

It should be noted that, at less internal friction angles, this relationship is not true. Hence, for different values of the settlement with the permeability coefficient $H/D = 3$, the ground surface settlement was higher than the values for the settling with the other values with less permeability coefficient. Also, according to the results obtained from A, with increasing penetration in the soil, the higher the permeability coefficient in the soil, the higher the saturation value of the soil, approaching the same trend for the other depths. Another point is that, with respect to the values in Table 3, the amount of settlement for the values of H/D and k, especially for the values obtained in $H/D = 2$ and $H/D = 3$, are almost equal in all cases and follow a similar

Table 3 Ground surface settlement in various modes

	c'	ϕ'				
		20°	30°	35°	40°	45°
$H/D=3$						
$k=1\times10^{-2}$ (m/s)	20 KPa	33.57	22.83	21.12	20.19	19.77
	40 kPa	24.74	19.84	18.87	18.33	18.08
	60 kPa	20.84	18.13	17.57	17.26	17.11
	80 kPa	18.63	17.03	16.70	16.51	16.44
$k=1\times10^{-5}$ (m/s)	20 KPa	33.36	22.71	21	20.07	19.62
	40 kPa	24.62	19.74	18.77	18.24	17.95
	60 kPa	20.74	18.04	17.47	17.17	17.01
	80 kPa	18.57	16.95	16.61	16.83	16.35
$k=1\times10^{-8}$ (m/s)	20 KPa	–	–	–	–	–
	40 kPa	37.57	23.62	20.15	17.52	15.8
	60 kPa	25.21	17.87	15.85	14.32	13.05
	80 kPa	18.96	14.70	13.41	12.73	12.02
$H/D=1$						
$k=1\times10^{-2}$ (m/s)	20 KPa	35.34	32.74	28.04	26.57	26.21
	40 kPa	21.38	18.07	17.65	17.61	17.81
	60 kPa	15.74	15.21	15.32	15.56	15.91
	80 kPa	15.51	13.81	14.10	14.45	14.85
$k=1\times10^{-5}$ (m/s)	20 KPa	23.32	25.64	24.38	22.38	21.88
	40 kPa	21.06	17.88	17.52	17.38	17.55
	60 kPa	15.58	15.04	15.24	15.38	15.70
	80 kPa	13.40	13.67	13.93	14.30	14.68
$k=1\times10^{-8}$ (m/s)	20 KPa	–	–	–	–	–
	40 kPa	20.15	16.28	14.7	13.60	13.26
	60 kPa	13.15	11.6	11.5	11.70	11.50
	80 kPa	9.64	10	10.5	10.80	11.22
$H/D=2$						
$k=1\times10^{-2}$ (m/s)	20 KPa	39.37	32.36	22.08	21.26	21.06
	40 kPa	23.37	23.97	18.37	18.07	18.04
	60 kPa	15.81	19.07	16.53	16.52	16.53
	80 kPa	16.04	16.76	15.45	15.45	15.78
$k=1\times10^{-5}$ (m/s)	20 KPa	38.92	23.79	21.90	21.07	20.86
	40 kPa	23.24	18.96	18.25	17.96	17.76
	60 kPa	18.39	16.66	16.41	16.40	16.40
	80 kPa	15.94	15.35	15.35	15.47	15.48
$k=1\times10^{-8}$ (m/s)	20 KPa	–	–	–	–	–
	40 kPa	32.70	20.54	17.69	15.30	14.42
	60 kPa	19.41	14.49	13.41	12.69	11.65
	80 kPa	13.51	11.91	11.40	10.99	10.94

trend. It seems that more decreasing permeability values will not have a significant effect on the ground settlement.

4.2 Investigation of the effect of adhesion changes in soil

By increasing the values obtained from Table 3 and Fig. 5, the increase in adhesion in all scenarios and analyses has reduced the amount of ground settlement. However, as illustrated in Fig. 5, as the internal friction angle of the soil increases, their corresponding points get closer to the center of the diagram, indicating a decrease in settlement at the surface as the soil adhesion increases. It can also be said that the trend of subsidence difference is more pronounced with the simultaneous change of soil adhesion and internal friction angle at lower depths, for values of $H/D = 1$ and $H/D = 2$ than in the other case.
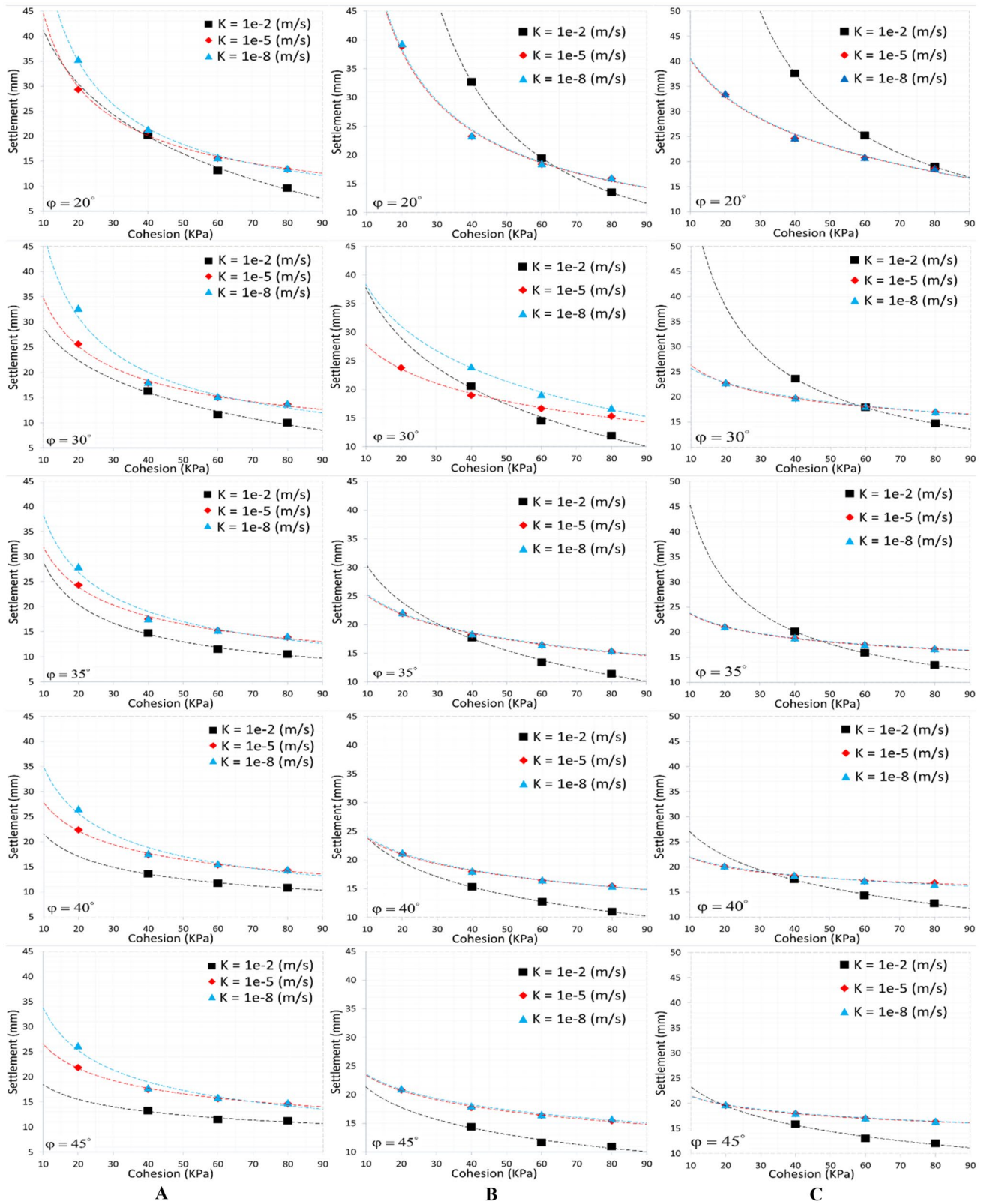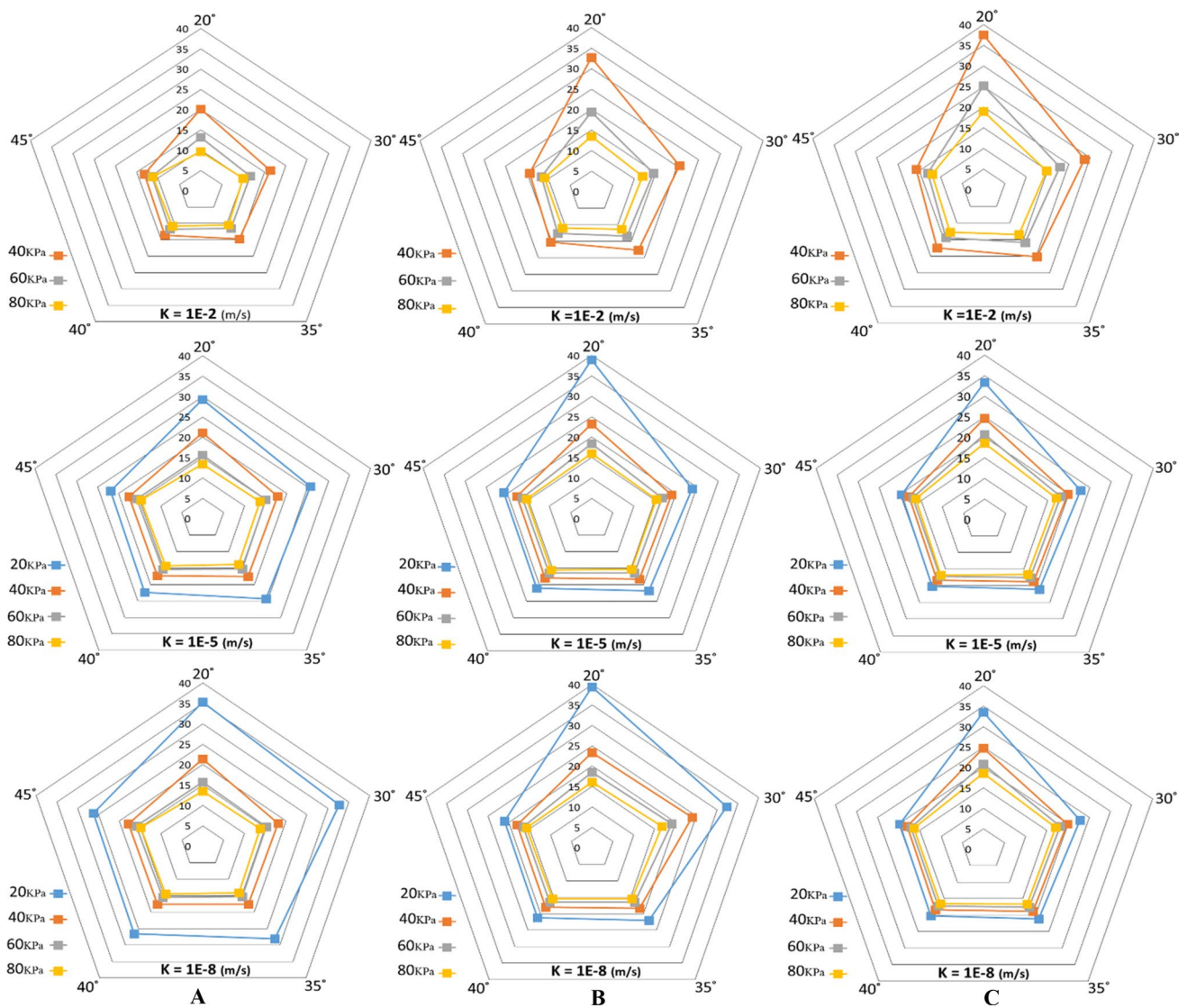
Fig. 4 Ground surface settlement curve for different permeability coefficients in three depths: **a** $H/D = 1$, **b** $H/D = 2$, **c** $H/D = 3$
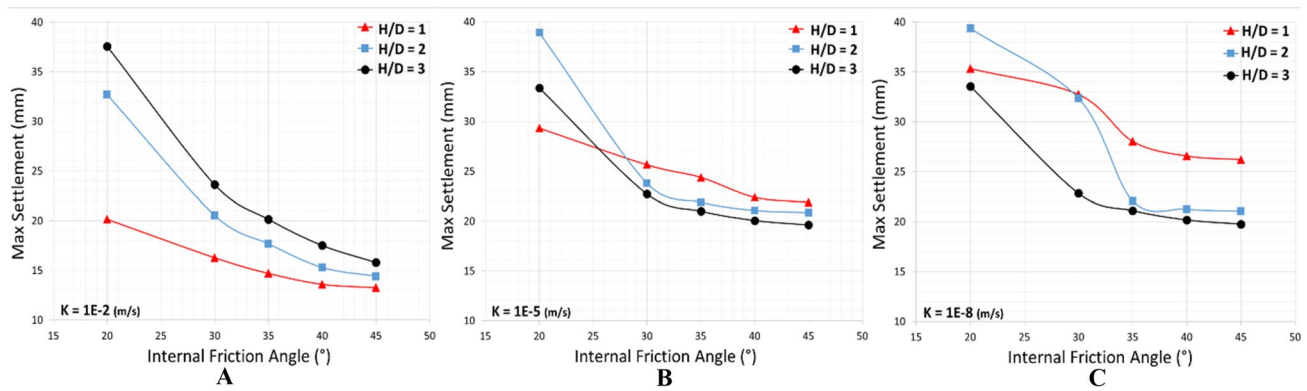
Fig. 5 Ground surface settlement curve for different Cohesion strength in three depths: **a** $H/D = 1$, **b** $H/D = 2$, **c** $H/D = 3$

In this section, the simultaneous influence of the geometrical parameters of the tunnel depth and diameter is simultaneously observed and investigated. The ground surface behavior due to tunneling at different depths is not the same. As shown in Table 3 and the diagrams in Fig. 6, the influence of tunneling depth on the ground surface settlement cannot be conclusively commented. This means that the ground surface settlement at different depths is completely dependent on the shear strength parameters of the soil.

When the permeability coefficient is highest and the internal friction angle of the soil is at its lowest, the ground surface settlement is a function of depth that has increased markedly with increasing subsurface depth. However, with increasing soil shear strength

parameters, the dependence of the ground surface settlement on the depth is seen to be less so that when these parameters reach their maximum, it can be said that the ground settlement is independent of the depth of drilling. However, by decreasing the permeability coefficient in the soil, in almost all cases, when the internal friction angle is at its maximum, the ground settlement is independent of depth and converges to a constant settlement value at all depths. Increasing the angle of internal friction at these depths seems to have little effect on the settlement. But when soil adhesion and soil permeability coefficients are at their lowest value, the amount of ground settlement obtained increases with the approaching ground surface and decreases with increasing depth.

Fig. 6 Maximum ground surface settlement curve for three depths with different Cohesion strengths in three permeability coefficients: **a** $k = 1e - 2$, **b** $k = 1e - 5$, **c** $k = 1e - 8$

4.3 Investigation of the effect of internal friction angle of soil

It was expected that as the angle of internal friction increased and the density of soil particles increased, the amount of ground surface settlement caused by tunneling would decrease. According to the results of Table 3 and Fig. 6, with increasing soil internal friction angle, in most cases this decreasing trend for surface settlement is obtained. However, as the amount of soil adhesion increased simultaneously, this trend decreased, and in the analyses with greater adhesion, the difference between the maximum and minimum of settlement values for the different values of the internal friction angle was less.

Therefore, in some cases for adhesions larger than 40 kPa, as the internal friction angle of the soil increased, the surface settlement increased or was constant. This trend has been observed for tunnels closer to ground level. In general, the decrease in ground settlement due to the increase in the internal friction angle of the soil is evident for all three values of soil permeability coefficient and for tunnels with greater depth. Figure 7 shows the maximum settlement value for all three depths and in the three permeability coefficients, and as the angle of internal friction increases, the downward trend of the ground settlement was observed.

5 Artificial neural networks

The application of artificial neural networks and their advantages in numerical modeling has been discussed by many researchers [38, 39]. As regards, the purpose of the study was to predict the maximum of ground surface settlement. The neural network was used because of the high capability of the prediction model. Also, the maximum variation affecting soil behavior during tunneling, which included geometrical and soil mechanical variables, was used as input variables in the model. In general, it can be said that the artificial neural network is a model of the human brain, except that its speed is much higher than that of the human brain. Neural networks first process data by analyzing the relationship between data, and after the learning process, with high power and speed. Artificial neural networks that are used for prediction usually include an input layer, an output layer, and one or more middle layer. The network used in this study is a powerful multilayer perceptron network that has high power in predicting the desired variable. Each layer consists of nodes or nodes, also known as neurons. In the input layer, each node represents an independent variable, and in the output layer of each node, it represents a variable or dependent variable. The master brain of any neural network is the middle layer of that network. In fact, all math operations are done on this layer or layers. That is, each neuron in the input layer connects to all the middle layer (hidden layer) neurons through a connector. Each neuron in the middle layer stores the weighted variables of the input layer and adds them together. Then, a predetermined function designed by the user and known as the activating function calculates the desired output variable by applying the sum of the neurons. During the design of the network, the mean square error estimation criterion was used to calculate the error generated in the network and evaluate its optimal performance in predicting the dependent variable. Another criterion is also called the root mean square error. This criterion more clearly represents the amount of errors. In fact, the lower this value and the closer to zero, the neural network predicts the value of the dependent variable more accurately. The relationship between mean square error and root mean square error is given in Eqs. 3 and 4 [40].

In recent years, outcome prediction models using artificial neural network and multivariable logistic regression
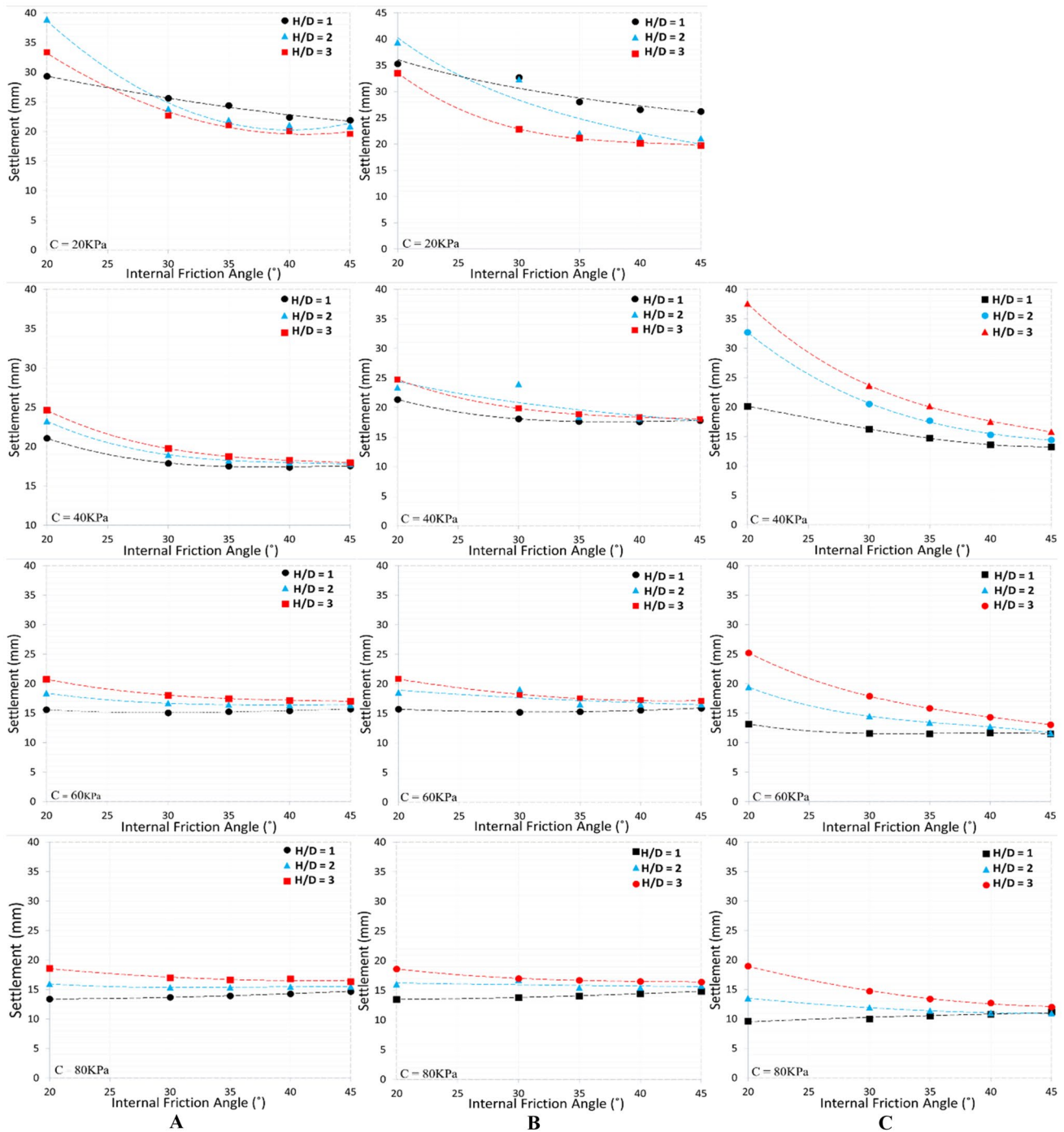
Fig. 7 Ground surface settlement curve for different cohesion strengths in three depths: **a** $k = 1e - 8$, **b** $k = 1e - 5$, **c** $k = 1e - 2$

analysis have been developed in many areas of engineering research. Both these methods have advantages and disadvantages. Artificial neural networks are algorithms that can be used to perform nonlinear statistical modeling and provide a new alternative to logistic regression, the most commonly used method for developing predictive models for engineering purposes. Neural networks offer a number of advantages, including requiring less formal statistical training, ability to implicitly detect complex nonlinear relationships between dependent and independent variables, ability to detect all possible interactions between predictor variables, and the availability of multiple training algorithms. Disadvantages include its "black box" nature, greater computational burden, proneness to

overfitting, and the empirical nature of model development. An overview of the features of neural networks and logistic regression is presented, and the advantages and disadvantages of using this modeling technique are discussed [41, 42].

$$\text{MSE} = \frac{1}{n} \sum_{i=1}^{n} \left(Y_i - \hat{Y}_i \right)^2 \qquad (3)$$

$$\text{RMSE} = \sqrt{\frac{1}{n} \sum_{i=1}^{n} \left(Y_i - \hat{Y}_i \right)^2} \qquad (4)$$

where n is the number of data, b is the value of calculating dependent variable and b is the value of dependent variable predicted by the network. When the measured error reaches its minimum value, the network will show better performance. The network error is calculated based on a set of algorithms that are created by the user when designing.

A common way to improve the network and reduce the error in the MLP network is to use a feedforward algorithm. In this way, the data series are divided into three categories: training data, evaluation data, and test data.

The value of the allowed error (minimum computational error) is also determined by the user. In the training data series, after the output of this data is obtained, this value is compared with the actual value and its difference is determined as a network error. Then, this error value is distributed over the weighted connections between the input and the middle layer to reduce the error and this process continues until the network reaches the minimum possible error. In Table 4 the input layer variables are shown as independent variables. Also, the output layer variable (ground surface settlement) is defined as the dependent variable. In this research, after data handling in ABAQUS, ground surface settlement prediction model using an MLP artificial neural network has been created, in which, according to Table 5, 70% of the data series are considered as training data, 15% for the evaluation data, and 15% for the testing data.

The Levenberg–Marquardt algorithm is also used to train the network and reduce the computational error. The Levenberg–Marquardt algorithm is used to solve nonlinear least-squares problems. The schematic diagram of the MLP artificial neural network is illustrated in Fig. 8. Among the different ways for artificial neural network

Table 5 Input variables of ANN

Parameter	Unit	Value
Crown depth-to-diameter ratio	H/D	1, 2, 3
Coefficient of permeability	$k(m/s)$	$1*10^{-8}, 1*10^{-5}, 1*10^{-2}$
Angle of internal friction	$\varphi(-)$	20, 30, 35, 40, 45
Cohesive strength	$C(kPa)$	20, 40, 60, 80

training in feedforward backpropagation methods, the Levenberg–Marquardt algorithm has been chosen for use in the present study because of its faster convergence in the training of medium-sized networks.

In this division, the parameter x_1 represents the diameter of the tunnel, x_2 represents the distance from the center to the center of the tunnels, x_3 shows the depth of the center of the second tunnel from the ground, and Y represents the maximum settlement of the earth's surface. Figure 8 shows the general structure of the network designed in this study, which uses the post-diffusion algorithm.

The design network consists of an input layer, an output layer, and a hidden layer with 7 nodes or neurons. The w_{11} represents the weighted connection of the first input to the first layer of the hidden layer. The w_{11} also indicates the weighted connection of the node or node of the output layer to the first hidden node. The w_{73} connection indicates the weighted connection of the third node or the neuron of the input layer to the seventh node or the hidden layer of the neuron. The w_{17} connection also shows the connection of the seventh neuron or the node of the output layer to the neuron or the node of the output layer. The grid shown in Fig. 8 is an artificial multilayer artificial neural network that uses a forward-looking post-propagation algorithm to reduce its error rate. The network uses the Marquardt–Levenberg law for its training phase. Also, the error calculation method is the MSE method, which calculates the error of each step of this method and is the main criterion for continuing the network training process. The data selection method is random in all three stages of network formation, which include training, evaluation, and network testing stages.

In each neural network, the number of middle layers and its neurons is usually determined and calculated according to the user experience as well as the number of input layer variables. This network contains seven neurons for the middle layer. The middle layer activator function

Table 4 Number of data and variables

All data	Training data	Evaluating data	Test data	Input variables	Output variables	Neuron of hidden layer
170	118	26	26	4	1	7

Fig. 8 General scheme of multilayer perceptron artificial neural network
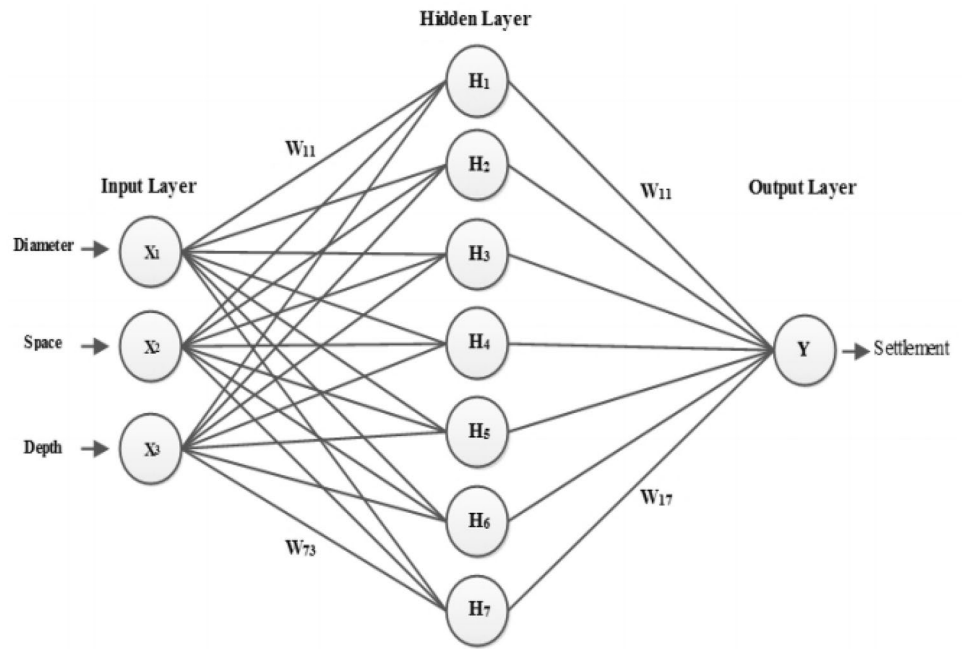
Table 6 Statistical results of ANN

Data categories	Correlation coefficient (R)	MSE	RMSE
Training data	0.99097	0.2932	0.5414
Evaluating data	0.95374	0.3564	0.5969
Test data	0.95415	0.3532	0.5943
All data	0.98409	0.3162	0.5623

is used in accordance with relation 5, which is called the sigmoid function. A linear function is also used to transfer the output from the middle layer to the last layer.

$$F(n) = \frac{1}{1 + e^{-n}} \tag{5}$$

The data and neurons of the multilayer perceptron neural network are presented in Table 5, which separately represents the number of data used in the different categories, the number of independent and dependent variables, and the number of neurons in the different layers.

Table 6 presents the statistical results of the artificial neural network, which shows the accuracy of the prediction of the dependent variable, which is ground surface settlement. The closer correlation coefficient (R) value to 1 indicates the linear relationship between the independent variables of the input layer and the dependent variable of the output layer.

Figure 9 shows the regression diagrams obtained for the training data sets, evaluation data sets, test data sets, and finally all data. The concentration of regression data

on the $x = y$ line indicates the highest power and accuracy of the network in predicting real values.

Table 7, in addition to the statistical results obtained from this study, compares the accuracy of the multilayer perceptron neural network with other intelligent networks and regression methods, where MLP is multilayer perceptron, ICA is an imperialist competitive algorithm, ANN is a new hybrid model of artificial neural network, MLR is multiple linear regression, and ABC is artificial bee colony.

6 Conclusion

In this study, parametric finite element analysis in ABAQUS software is carried out for investigating the ground surface settlement of a circular cross section single tunnel, with changes in geometrical characteristics such as diameter and depth of the tunnel (depth-to-diameter ratio) and changes in soil mechanical properties such as adhesion, internal friction angle, and soil permeability performed. Then, the values obtained for the surface settlement in different modes as dependent variables (output data) and four variables of adhesion, internal friction angle, permeability coefficient, and the depth-to-diameter ratio of the tunnel as independent variables (input data) are used to produce multilayer perceptron artificial neural network in MATLAB software. Multilayer perceptron artificial neural network, using the Levenberg–Marquardt error correction algorithm and using the feedforward backpropagation model, has demonstrated its ability to predict the surface settlement.
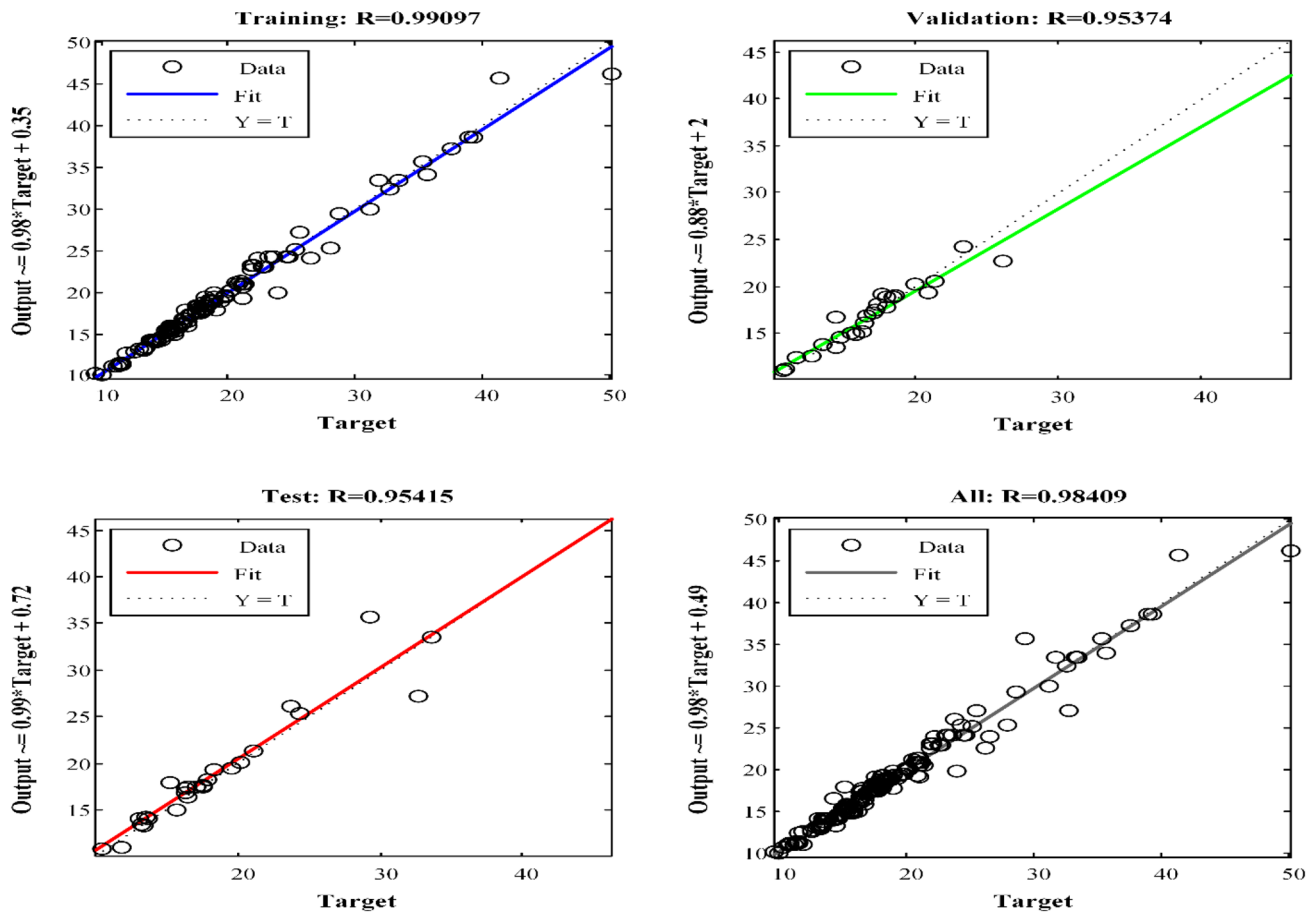
Fig. 9 Regression curve for different data in the MLP artificial neural network

Table 7 Comparison of the performance of different intelligent networks

Data categories	This study (MLP-ANN)	Moghaddasi et al. [35] (ICA-ANN)	Moghaddasi et al. [35] (ANN)	Moghaddasi et al. [35] (MLR)	Koopialipoor et al. [31] (ABC-ANN)
Training data	0.99097	0.9806	0.9402	0.9016	0.9351
All data	0.98409	09,729	0.9377	0.9036	0.9467

(1) The correlation and determination coefficients indicate the direct and linear relationship between the results obtained in the ABAQUS and the results of ANN. A comparison between this predictive model based on correlation coefficient (R) indices shows that the MLP-ANN with $R = 0.99097$ for training data and $R = 0.98409$ for all data is more accurate than the other intelligent network and regression models.

(2) All boundaries in each direction must have boundary conditions applied to them. If no boundary conditions are assigned to the model (free boundary), natural conditions apply. That is, the prescribed forces are equal to zero and the boundaries move freely. The software automatically sets a standard boundary to avoid the situation of indeterminate displacements, so that by designating reference points, the software completely rigs the horizontal boundary and by creating rolling boundaries in a vertical direction, it allows the soil to move and settle.

(3) The urban tunnel with no overburden is considered at ground surface, and the porosity ratio for the whole model is considered to be 0.58 with respect to its specific gravity and weight density of solid grains. The analysis is done in two steps. The first step includes entering the necessary information into the software, creating appropriate boundary conditions and applying pore water pressures and effective in situ stresses in the soil model, and then, performing drilling opera-

tions, in which, immediately after drilling, ground surface settlement values are measured

(4) Surface settlement and crown of the tunnel are directly related to the simultaneous increase in the diameter of tunnels. This means that increasing the diameter of the tunnels will increase the surface settlement and crown of the tunnel.

(5) When the tunnels are located closer to the ground, we see more settlements, both on the surface and in the crown of the tunnels; while increasing the depth, we saw a decrease in the settlement. This reduction in settlement continued until the depth-to-diameter ratio of the tunnel reached a certain value, and since then we have again seen an increase in the surface settlement and crown of the tunnels.

Compliance with ethical standards

Conflict of interest The authors declare that they have no competing interests.

References

1. Ghiasi V, Ghiasi S, Prasad A (2012) Evaluation of tunnels under squeezing rock condition. J Eng Des Technol 10(2):168–179. https://doi.org/10.1108/17260531211241167
2. Ghiasi V, Mozafari V (2018) Seismic response of buried pipes to microtunnelling method under earthquake loads. Soil Dyn Earthq Eng 113:193–201
3. Ghiasi V, Jalalvand A, Saeidijam S (2014) diaphragm wall-tunnel interaction in saturated Soil 2014. Electron J Geotech Eng 1(9):2669–2678
4. Ghiasi V, Omar H (2011) Analysis of shotcrete lining of underground tunnels. Pertanika J Sci Technol 19(2):249–257
5. Shui-Long S (2014) Huai-Na Wu, Yu-Jun Cui, Zhen-Yu Yin, Long-term settlement behaviour of metro tunnels in the soft deposits of Shanghai. Tunn Undergr Space Technol 40:309–323
6. Lai J, Qiu J, Feng Z, Chen J, Fan H (2016) Prediction of soil deformation in tunnelling using artificial neural networks. Comput Intell Neurosci. https://doi.org/10.1155/2016/6708183
7. Martos F (1958) Concerning an approximate equation of the subsidence trough and its time factor. In: Proceedings of the international strata control congress, Leipzig, 1958, pp 191–205
8. Peck R (1969) Deep excavations and tunnelling in soft ground. In: Proceedings of the 7th international conference on soil mechanics and foundation engineering, Mexico, Mexico City, pp 225–290
9. O'Reilly M, New B (1982) Settlements above tunnels in the United Kingdom, their magnitude and prediction. In: Proceedings of the tunnelling '82 Inst of Mining & Metallurgy, Brighton, pp 173–181
10. Suwansawat S, Einstein HH (2007) Describing settlement troughs over twin tunnels using a superposition technique. J Geotech Geoenviron Eng 133:445–468
11. Yang X, Wang J (2014) Ground movement prediction for tunnels using simplified procedures. Tunn Undergr Space Technol 26:462–471
12. Fang Y, Wu C, Chen S, Liu C (2014) An estimation of subsurface settlement due to shield tunneling. Tunn Undergr Space Technol 44:121–129
13. Park K (2005) Analytical solution for tunnelling-induced ground movement in clays. Tunn Undergr Space Technol 20:249–261
14. Yang X, Wang JM (2011) Ground movement prediction for tunnels using simplified procedure. Tunn Undergr Space Technol 26:462–471
15. Saeid R, Dindarloo E (2015) Maximum surface settlement based classification of shallow tunnels in soft ground. Tunn Undergr Space Technol 378(19):4–5
16. Abdellah W, Ali MA, Yang H-S (2018) Studying the effect of some parameters on the stability of shallow tunnels. J Sustain Min 17(1):20–33
17. Idinger G, Aklik P, Wu W, Borja RI (2001) Centrifuge model test on the face stability of shallow tunnel. Acta Geotech 6:105–117
18. Chapman D, Rogers CDF, Hunt DVL (2004) Predicting the settlements above twin tunnels constructed in soft ground. Tunn Undergr Space Technol 378(19):4–5
19. Ng C, Hong Y, Soomro M (2015) Effects of piggyback twin tunnelling on a pile group: 3D centrifuge tests and numerical modelling. Geotechnique 65(1):38–51
20. Kirsch A (2010) Experimental investigation of the face stability of shallow tunnels in sand. Acta Geotech 5(1):43–62
21. Divall S, Goodey R, Taylor R (2012) Ground movements generated by sequential twin-tunnelling in over-consolidated clay. Geotechnical Engineering Research Group, City University, London
22. Sams M (2013) Numerical and physical modelling of a 2D tunnel heading at collapse. University of Southern Queensland Bachelor Research Project, Queensland
23. Mödlhammer H (2010) Numerical methods for tunneling using ABAQUS and investigations of long-time-effects of the shotcrete shell and its impact on the combined support system. Master Thesis, MIT
24. Karakus M (2007) Appraising the methods accounting for 3D tunnelling effects in 2D plane strain FE analysis. Tunn Undergr Space Technol 22(1):47–56
25. Karakus M, Fowell RJ (2005) Back analysis for tunnelling induced ground movements and stress redistribution. Tunn Undergr Space Technol 20(6):514–524
26. Shahrour I, Mroueh H (1997) Three-dimensional nonlinear analysis of a closely twin tunnel. In: Sixth international symposium on numerical models in Geomechanics, (NUMOG VI)
27. Addenbrooke T, Potts DM, Puzrin AM (1997) The influence of pre-failure, soil stiffness on the numerical analysis of tunnel construction. Geotechnique 47(3):693–712
28. Pakbaz M, Imanzadehb S, Bagheriniac K (2013) Characteristics of diaphragm wall lateral deformations and ground surface settlements: Case study in Iran-Ahwaz metro. Tunn Undergr Space Technols 35:109–121
29. Baziar M, Rabeti M, Choo Y, Kim D (2016) Tunnel flexibility effect on the ground surface acceleration response. Earthq Eng Eng Vib 15(3):457–476
30. Priddy K, Keller PE (2005) Artificial neural networks: an introduction. SPIE press, Bellingham
31. Koopialipoor M, Ghaleini EN, Tootoonchi H, Armaghani DJ, Haghighi M, Hedayat A (2019) Developing a new intelligent technique to predict overbreak in tunnels using an artificial bee colony-based ANN. Environ Earth Sci 78(5):165
32. Hajihassani M, Armaghani DJ, Sohaei H, Mohamad ET, Marto A (2014) Prediction of airblast-overpressure induced by blasting

using a hybrid artificial neural network and particle swarm optimization. Appl Acoust 80:57–67

33. Ocak I, Seker SE (2013) Calculation of surface settlements caused by EPBM tunneling using artificial neural network, SVM, and Gaussian processes. Environ Earth Sci 70(3):1263–1276

34. Suwansawat S, Einstein HH (2006) Artificial neural networks for predicting the maximum surface settlement caused by EPB shield tunneling. Tunn Undergr Space Technol 21(2):133–150

35. Moghaddasi MR, Noorian-Bidgoli M (2018) ICA-ANN, ANN and multiple regression models for prediction of surface settlement caused by tunneling. Tunn Undergr Space Technol 79:197–209

36. Chen RP, Zhu J, Liu W, Tang XW (2011) Ground movement induced by parallel EPB tunnels in silty soils. Tunn Undergr Space Technol 26(1):163–171

37. Yamamoto K, Lyamin AV, Wilson DW, Sloan SW, Abbo AJ (2011) Stability of a circular tunnel in cohesive-frictional soil subjected to surcharge loading. Comput Geotech 38(4):504–514

38. Maleki E, Unal O (2020) Fatigue limit prediction and analysis of nano-structured AISI 304 steel by severe shot peening via ANN. Eng Comput. https://doi.org/10.1007/s00366-020-00964-6

39. Maleki N, Kashanian S, Maleki E, Nazari M (2020) A novel enzyme based biosensor for catechol detection in water samples using artificial neural network. BEJ. https://doi.org/10.1016/j.bej.2017.09.005

40. Shiau J, Sams M, Zhang J, Kemp R (2014) Settlement analyses of underground circular tunneling in soft clay. In: Geotechnical aspects of underground construction in soft ground, pp 347–52

41. Tu V (1996) Advantages and disadvantages of using artificial neural networks versus logistic regression for predicting medical outcomes. J Clin Epidemiol 49(11):1225–1231. https://doi.org/10.1016/S0895-4356(96)00002-9

42. Eftekhar B, Mohammad K, Ardebili HE, Ghodsi M, Ketabchi E (2005) Comparison of artificial neural network and logistic regression models for prediction of mortality in head trauma based on initial clinical data. BMC Med Inform Decis Mak. https://doi.org/10.1186/1472-6947-5-3

Publisher's Note Springer Nature remains neutral with regard to jurisdictional claims in published maps and institutional affiliations.